PETROLOGY OF THE CLOTTY GRANITE, PERRAULT FALLS, ONTARIO

A Thesis Submitted to
The Faculty of Graduate Studies
University of Manitoba

In partial fulfillment
of the requirements for the degree
Master of Science

by
James Arthur Morin
September 1970

ABSTRACT

A granite at Perrault Falls, Ontario, is characterized by clots of biotite and sillimanite which are disseminated within a garnetiferous granitic matrix. The clots are surrounded by leucocratic rims. A disturbed relict foliation is present in the arrangement of the clots. The granite shows intrusive relationships with the neighbouring paragneisses.

Ternary variation diagrams reveal that the clotty granite and the neighbouring granites represent different stages of partial melting of gneisses. Green and brown biotites in the clotty granite have different compositions because of different degrees of reaction with silicate melt. The iron-rich brown biotite suggests a minimum for the P-T environment of P=4 kb., T=640^{o}C. The garnet is almandine-rich pyralspite. The alkali feldspar of the clotty granite and neighbouring granites is intermediate to maximum microcline, while that of the gneisses is predominantly orthoclase.

The clotty granite was derived by the partial melting of layered paragneiss. Due to an increase in P_{H_2O} and temperature, the salic components of the gneiss melted, thus forming a melt with undigested melanocratic clots formed by the disintegration of the biotite-rich layers. The mixture of melt and clots was then injected into its present intrusive position, without completely mixing the relict layers of mafic minerals.

TABLE OF CONTENTS

LIST OF FIGURES

List of Figures (cont'd)

L I S T O F T A B L E S

INTRODUCTION

The clotty granite occurs in the Perrault Falls area of Northwestern Ontario, about 60 miles north of Vermilion Bay (see Figure 1). The location of examined outcrops of the clotty granite is shown in Figure 2. The amount of bedrock outcrop is small, much of the area being covered by Pleistocene glacial deposits of sand and silt.

The area is characterized by granites and high grade regionally metamorphosed gneisses and migmatites of the English River Gneissic Belt. The clotty granite shows evidence of an intrusive origin. The gneissosity of the paragneisses is mildly deformed at the contact with the clotty granite, indicating a forceful intrusion of the clotty granite (see Figures 3 and 4).

The clotty granite consists of clots of biotite and sillimanite distributed within a granitic matrix. The texture and mineralogy of the matrix indicates crystallization from an igneous melt. On the other hand, the clots have a metamorphic texture and mineralogy. They are interpreted to be relicts of melanocratic biotite-rich layers of paragneisses that have escaped melting. The field evidence, petrography, mineralogy and chemical composition all point to an origin of the clotty granite by partial melting or partial anatexis of paragneisses.

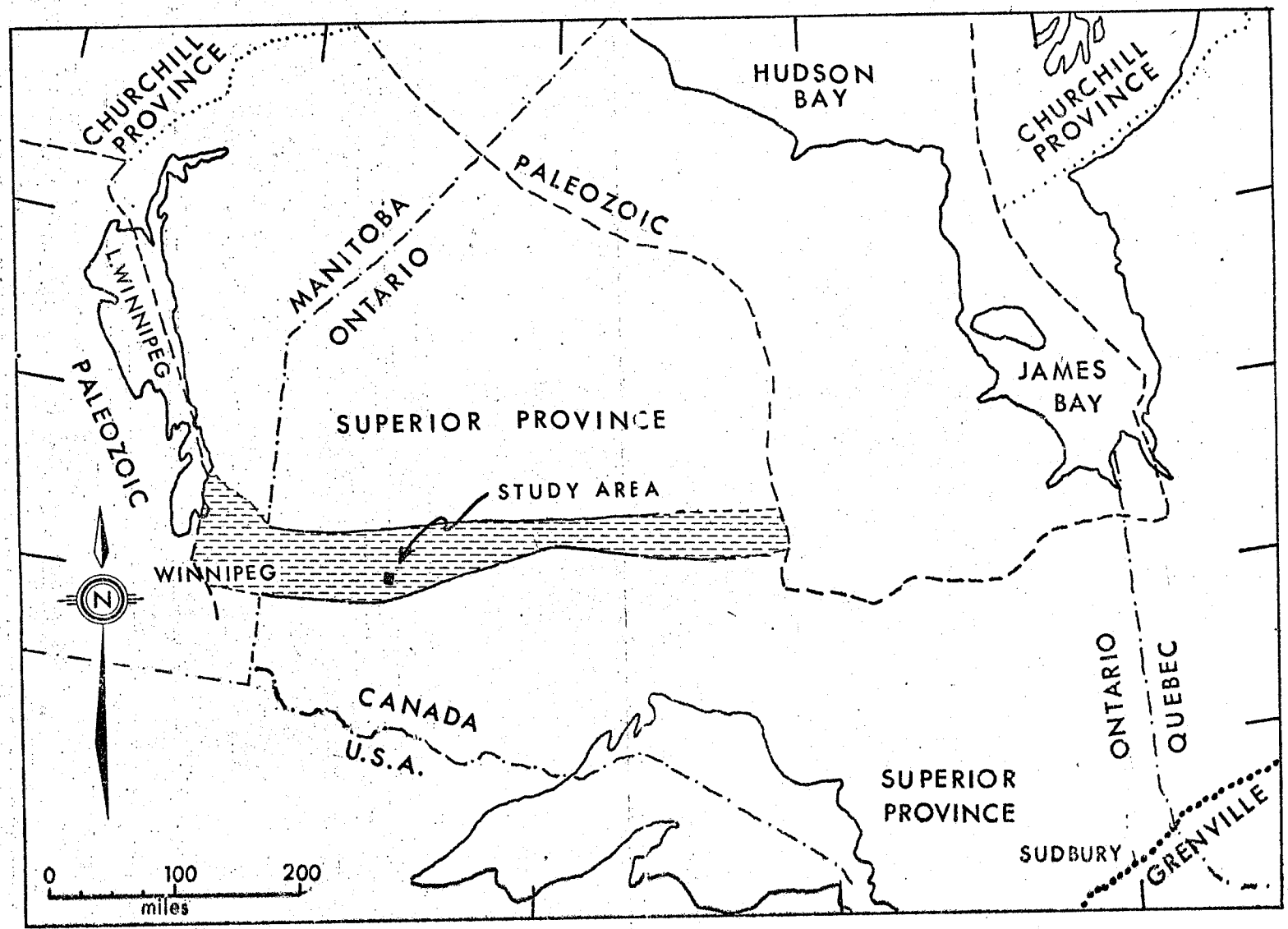

Fig. 1. Location of the study area at Perrault Falls, Ontario. The area marked by a dashed pattern is the English River Gneissic Belt (after Wilson & Brisbin, 1963).

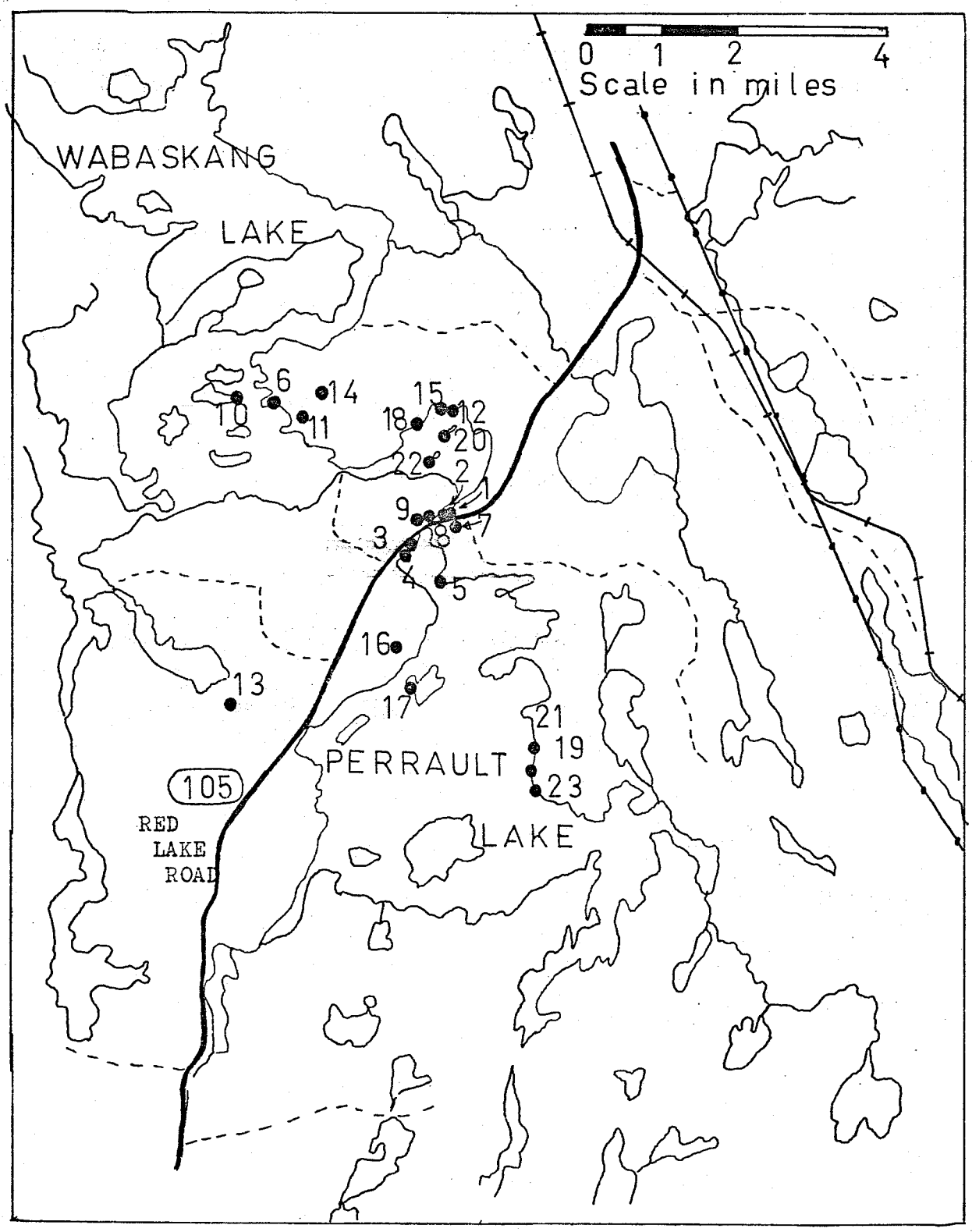

Figure 2 Map of thesis area with sample locations marked.

REGIONAL CRUSTAL STRUCTURE

The study area lies within the English River Gneissic Belt of the Superior Province as defined by Wilson and Brisbin (1963) (see Figure 1). The English River Gneissic Belt is composed mainly of highly metamorphosed metasedimentary rocks and granitic rocks. It has been interpreted by Wilson and Brisbin (1963) as an uplifted block of the lower levels of the granitic crust. It truncates the southeast-trending axes of the older volcanic-granitic rocks to the north and is in fault contact with the group of the Keewatin belt of lavas and the Quetico Belt of metasedimentary rocks to the south. Dwibedi (1966) found that within the English River Gneissic Belt, the grade of metamorphism decreased from the granulite facies in the south to the lower amphibolite facies in the north along Highway 105. Numerous paragneiss domes occur near the area.

GENERAL GEOLOGY

The main rock types of the study area are paragneiss, granite and pegmatite. The paragneisses are intruded by the clotty granite, granites and pegmatites. Contact relationships include deformation of gneissic structure in the paragneiss, and xenoliths of paragneiss in granite. No basic intrusions were found.

STRUCTURAL FEATURES

Outcrops of the clotty granite are scarce, and because of this, no definite shape can be assigned to it. In places, it occurs as a thin dike intrusive into the paragneisses, and thus the clotty granite may exist as numerous separated small pegmatite-like intrusions into the paragneisses. The contact of the clotty granite and the paragneiss was observed on a major hill outcrop northeast of Wabaskang Lake (see Figure 3). The contact is sharp and no chilled margin features occur. The gneissosity in the paragneiss is deformed and the deformation is interpreted to reflect a forceful intrusion of the clotty granite into the paragneiss.

The clots range in size from 0.5 inches to about 6 inches in length, and up to 1 inch in thickness. They are irregularly shaped, but approximate a disc shape. Differential weathering of the clotty granite results in the clots appearing as small pits in places (see Figure 4). The clots are locally homogeneously distributed within a coarse-grained garnetiferous granite matrix. In one outcrop, the clots are surrounded by leucocratic haloes about 0.5 inches in width (see Figure 5). The clots are foliated in places and the foliation has a trend which is parallel to that of the local paragneisses (see Figure 6). In places, the foliation exhibits a flexure which is interpreted as due to flow in a semi-fluid medium (see Figure 7). At one locality, the clots themselves appear to be flexed or drag folded in response to differential flow in a semi-fluid medium (see Figure 5). The foliation resembles a relic gneissosity in places (see Figure 8).

Figure 3a. Contact between clotty granite and paragneiss north of Wabaskang. (Location 6).

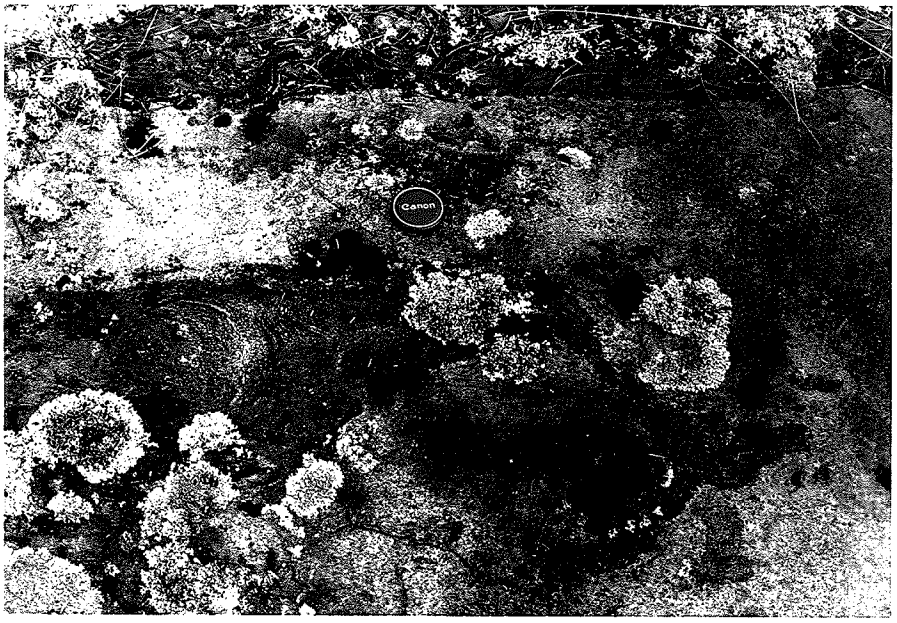

Figure 3b. Contact as above. Note distortion of foliation in paragneiss. (Location 6).

Figure 4. Photograph of clotty granite showing differential weathering of clots. Outcrop is on south side of Highway 105. (Location 7).

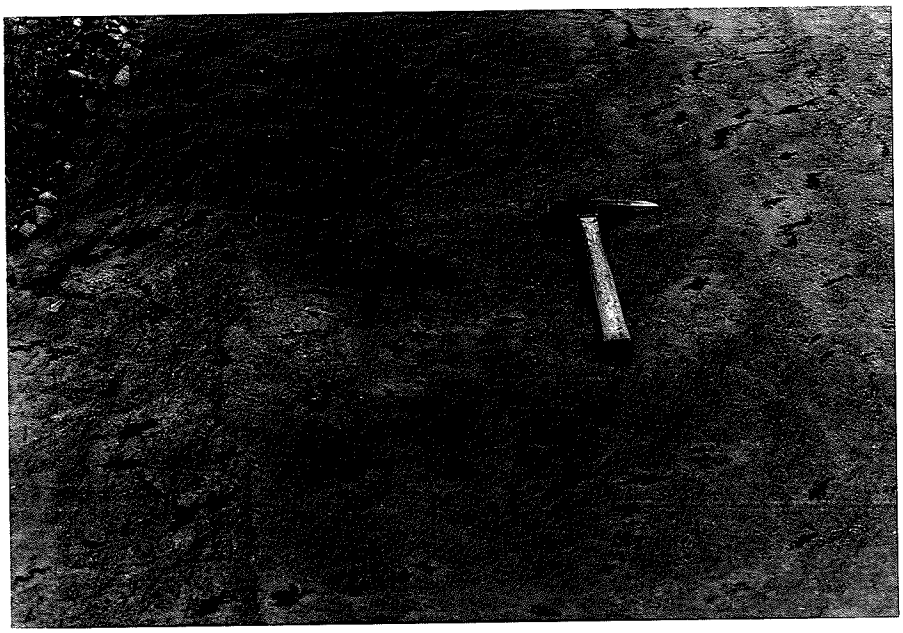

Figure 5. Clotty granite west of Perrault Falls; note "s" shaped clots and leucocratic haloes around clots; clots are foliated toward upper right corner of photograph. (Location 8).

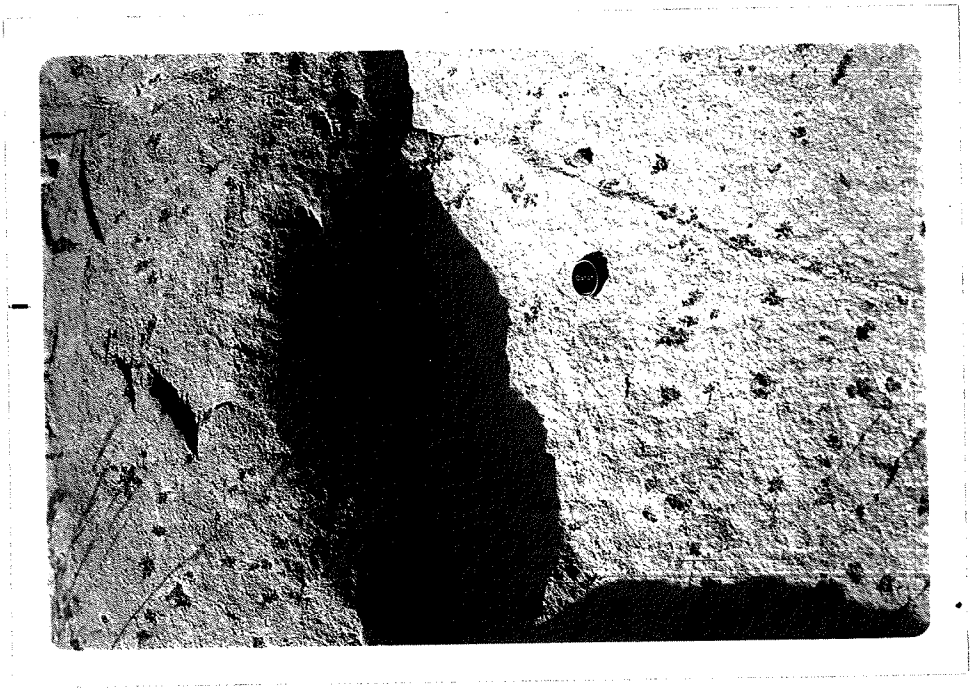

Figure 6. Clotty granite on Red Lake Road showing foliation of clots. (Location 1).

Figure 7. Gently deflected layers of clots in clotty granite west of Perrault Falls; flexure due to flow. (Location 8).

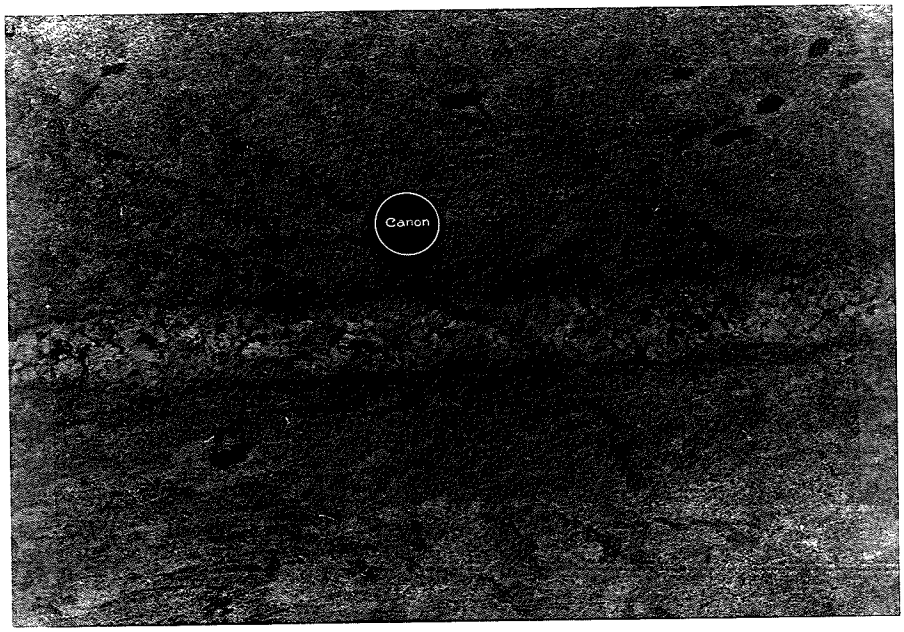

Figure 8. Pegmatite within clotty granite west of Perrault Falls. Note leucocratic haloes around clots in upper right. Also note the gneissic layering in lower left. (Location 9).

Figure 9a. Photograph of clotty granite showing clots and irregular trending pegmatites with some included clots. (Location 1).

Figure 9b. Photograph of clotty granite showing clots and small pegmatite lenses. (Location 1).

Figure 9c. Clotty granite with irregularly trending pegmatite containing clots. (Location 1).

The clotty granite is also characterized by irregular trending pegmatite veinlets within it. Clots and garnets occur in some of these veinlets (see Figure 9 a,b,c). The veinlets are smaller than 6 inches in width. Some of them consist of a blocky alkali-feldspar-quartz border and a quartz core (see Figure 10). Alkali feldspar megacrysts also occur in the clotty granite (see Figure 11).

PARAGNEISS

The paragneiss of the area is intruded by the granites and pegmatites, in addition to the clotty granites (see Figure 12). The paragneiss has mostly a gneissose structure consisting of alternating leucocratic and melanocratic thin bands of feldspar-quartz and feldspar-biotite-quartz respectively. Interlayered biotite schist and amphibolite occur in places. Lit-par-lit type pegmatites also occur. The paragneiss is intensely folded in places and appears to have been partly mobilized in some areas (see Figure 13 a,b). This partial mobilization may be an intermediate step to the formation of a clotty granite.

GRANITE AND PEGMATITE

The granites and pegmatites of the area are all coarse-grained. They range from white to pink in colour. Xenoliths of paragneiss were observed in places and this indicated that the granites were intrusive into the paragneisses,(see Figure 14). The granitic rocks were subjected to several periods of remobilization as indicated by "meta-basite" type intrusive-intruded relationships with other granites (see Figure 15).

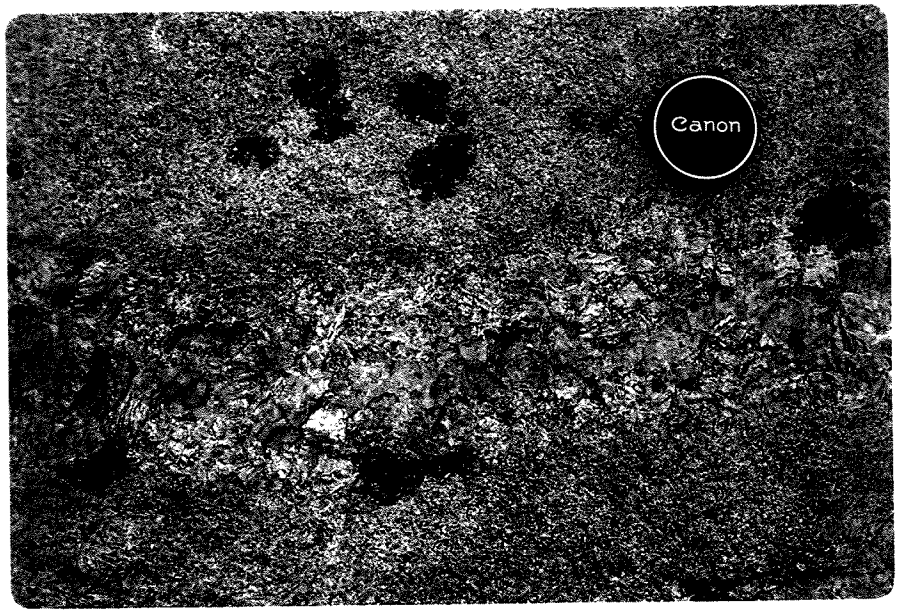

Figure 10. Photograph of pegmatite in clotty granite. Note blocky feldspar-quartz margin and quartz core; illustrates physical segregation of growing crystalline phases precipitated from an aqueous melt. (Location 1).

Figure 11. K-feldspar megacryst within clotty granite south of Red Lake Road and east of Perrault Falls. (Location 7).

Figure 12. Wedge of paragneiss projecting into coarse grained granite northeast of Wabaskang Lake. (Location 14).

Figure 13a. Partially melted and highly contorted paragneiss; possible intermediate stage to evolution of the clotty granite. (Location 14).

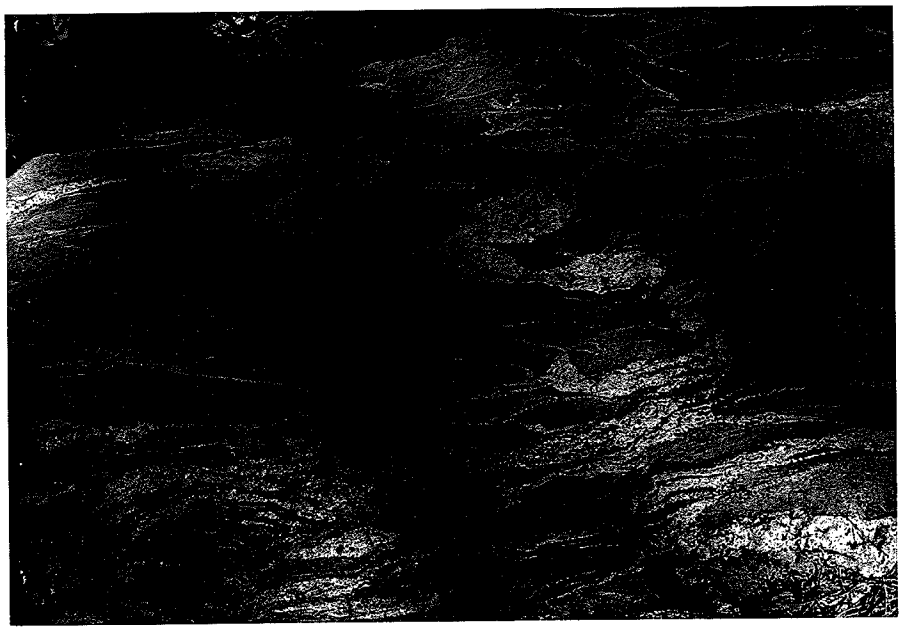

Figure 13b. Contorted veins of leucocratic material within paragneiss northeast of Wabaskang Lake. (Location 14).

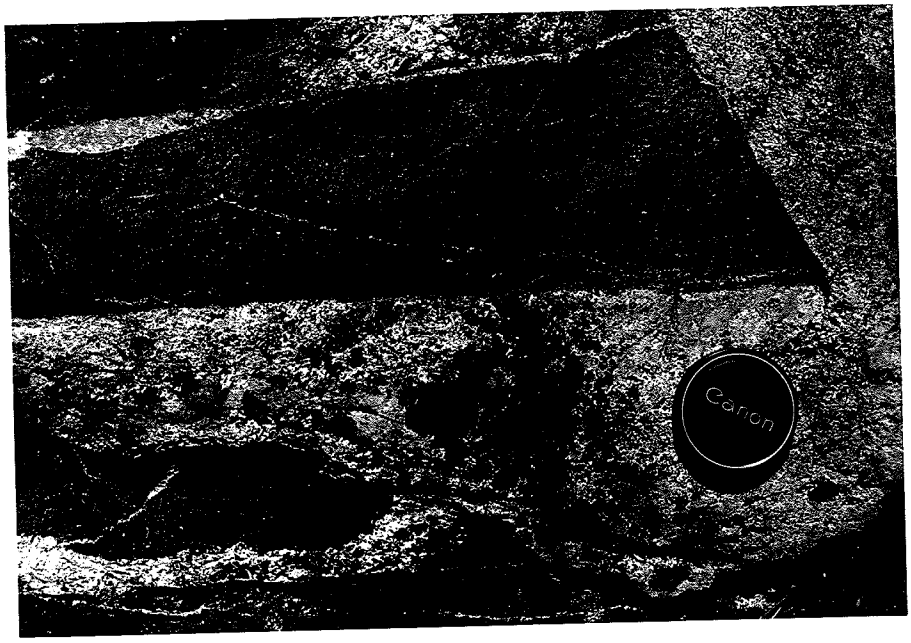

Figure 14. Photograph of biotite schist xenoliths within granite west of Perrault Lake. (Location 16).

Figure 15. Photograph of biotite granite intruded into pegmatite on island in Central Wabaskang Lake. Remobilization of pegmatite has resulted in intrusive relations of pegmatite to biotite granite. (Location 10).

COMPOSITION

CLOTTY GRANITE

The chemical compositions and Niggli norms of some clotty granites are given in Table 1. Exposures of the clotty granite northeast of Wabaskang Lake are highly weathered and thus were not chemically analysed. The concentration of clots in the clotty granite varies from outcrop to outcrop, and even within a single outcrop. The outcrops northeast of Wabaskang Lake have clot concentrations of about two to four percent (see Figure 3). In contrast, the outcrops near Perrault Falls have clot concentrations in the five to seven percent range (see Figure 16).

MATRIX

The granite matrix has a homogenous medium to coarse hypidiomorphic granular texture. It consists of the following minerals: microcline and microcline-perthite (75%), quartz (15%), plagioclase (5%), biotite (3%), garnet (3%), muscovite (2%), and very minor sillimanite, zircon, myrmekite and hematite.

The microcline and microcline-perthite are typically medium to coarse grained and slightly poikilitic. The microcline exhibits good M-twinning. Euhedral to subhedral inclusions of brown biotite, plagioclase and quartz can occur in these minerals (see Figure 17). Myrmekite also occurs as inclusions. Perthite albitic exsolution lamellae thicken towards the edges (see Figure 17). Rarely, biotite, muscovite, quartz or zircon may be concentrated at the intergranular boundry between two perthites. Sericite forms rare veinlets piercing the perthite. A few corroded grains of microcline, possible relict, occur as inclusion in plagioclase and perthite.

Quartz has more than one type of habit in the matrix. Medium-grained hexagonal dipyramids of quartz occur as inclusions in some of the perthite and microcline. In addition, coarse-grained anhedral intersertal quartz grains occur which, in some rocks, are crystallographically aligned parallel to each other. These intersertal grains have a distinctive, unstrained "fresh-looking" appearance and show textural relations which suggest they crystallized before some of

Figure 16. Clotty granite on Red Lake Road; Note pegmatite vein with included clots. (Location 1).

TABLE I

CHEMICAL ANALYSES:

	1-1W	1-1M	2-1W	2-1M	3-2W	3-2M
SiO_2	74.60	74.15	72.70	74.70	74.35	75.40
Al_2O_3	13.73	14.38	13.86	13.71	12.99	13.11
Fe_2O_3	0.35	0.39	0.91	0.10	0.18	0.04
FeO	0.81	0.60	0.02	0.24	0.29	0.14
MgO	0.28	0.12	0.30	0.08	0.37	0.22
CaO	0.76	0.84	1.40	1.72	2.22	2.27
Na_2O	3.90	4.35	4.13	4.02	4.41	4.05
K_2O	4.88	4.92	5.57	4.84	4.28	4.17
H_2O	0.37	0.23	0.44	0.12	0.30	0.03
CO_2	0.01	0.00	0.01	0.03	0.03	0.03
TiO_2	0.00	0.00	0.00	0.00	0.00	0.00
P_2O_5	0.24	0.22	0.20	0.20	0.17	0.18
MnO	0.01	0.02	0.04	0.00	0.01	0.01
TOTAL	99.94	100.22	99.68	99.76	99.60	99.65

NIGGLI NORMS:

Calcite	0.00	0.03	0.08	0.08	0.08
Apatite	0.46	0.00	0.42	0.36	0.38
Ilmenite	0.00	0.00	0.00	0.00	0.00
Orthoclase	29.12	33.30	28.81	25.50	24.86
Albite	39.04	37.45	36.28	39.84	36.60
Anorthite	2.73	2.81	5.06	2.99	5.28
Magnetite	0.41	0.41	0.10	0.19	0.04
Hematite	0.00	0.61	0.00	0.00	0.00
Corundum	0.96	0.00	0.00	0.00	0.00
Wollastonite	0.00	1.67	0.81	2.72	1.88
Enstatite	0.33	0.84	0.22	1.04	0.62
Ferrosilite	0.66	0.00	0.30	0.33	0.19
Quartz	26.28	23.27	27.91	26.96	30.08

LEGEND

1-1W, 2-1W, 3-2W - whole rock clotty granites, locations 1, 2, 3, respectively.
1-1M, 2-1M, 3-2M - clotty granite matrices, locations 1, 2, 3 respectively.

Analysts - K. Ramlal, University of Manitoba and J. Morin.

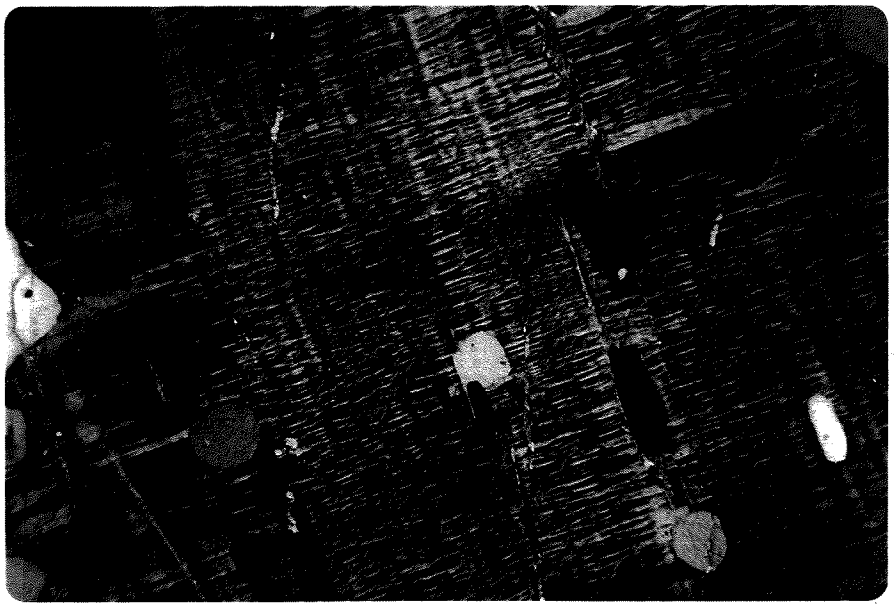

Figure 17. Photomicrograph of a part of a large perthite megacryst with thicker albite lamellae at the edge; inclusions of brown biotite and drop quartz; crossed nicols, X 76. (Location 2).

the microcline. Quartz also occurs as fine-grained anhedral aggregates associated with muscovite, sillimanite and fine-grained K-feldspar.

Biotite occurs scattered throughout the matrix as brown euhedral medium-grained crystals. In association with garnet, however, the biotite is mostly green and anhedral (see Figure 18). The brown biotite is present as inclusions within plagioclase, microcline and perthite. Biotite is in part replaced by microcline, with a rim of sericite developed between the microcline and the biotite. Muscovite also replaces the biotite.

Plagioclase occurs as medium-grained tabular subhedral grains, normally included in microcline and perthite. Albite twinning is generally poorly developed. Myrmekite consisting of intergrown albite and quartz may be associated with the plagioclase, mainly at contacts with quartz and microcline (see Figure 19).

Garnets occur sporadically throughout the matrix. They are coarse-grained,anhedral to subhedral, and are mostly associated with green biotite (see Figure 18). They are pink coloured and are almandine-rich. In some garnets, anhedral biotite inclusions are optically identical with each other. Anhedral fine-grained K-feldspar inclusions also occur within the garnets.

Muscovite occurs as fine to medium grained euhedral laths associated with biotite, microcline and microcline-perthite. A few muscovite grains contain fine-grained inclusions of quartz and hematite-ilmenite. The muscovite normally occurs in a replacement type texture, coherently pseudomorphous after biotite. It is, in part, replaced by a sillimanite and K-feldspar aggregate.

Sillimanite is a very minor constituent and occurs in bundle-shaped aggregates of fine-grainded fibrous sillimanite and K-feldspar which are non-coherently pseudomorphous after biotite and, in part, muscovite.

Zircon generally occurs as fine grained euhedral inclusions surrounded by strongly pleochroic haloes in biotite.

Hematite-ilmenite occurs as fine to very fine grained anhedral inclusions disseminated throughout some of the muscovite and biotite.

The chemical compositions and Niggli norms of the granite matrices labelled 1-1M, 2-1M and 3-2M are included in Table 1.

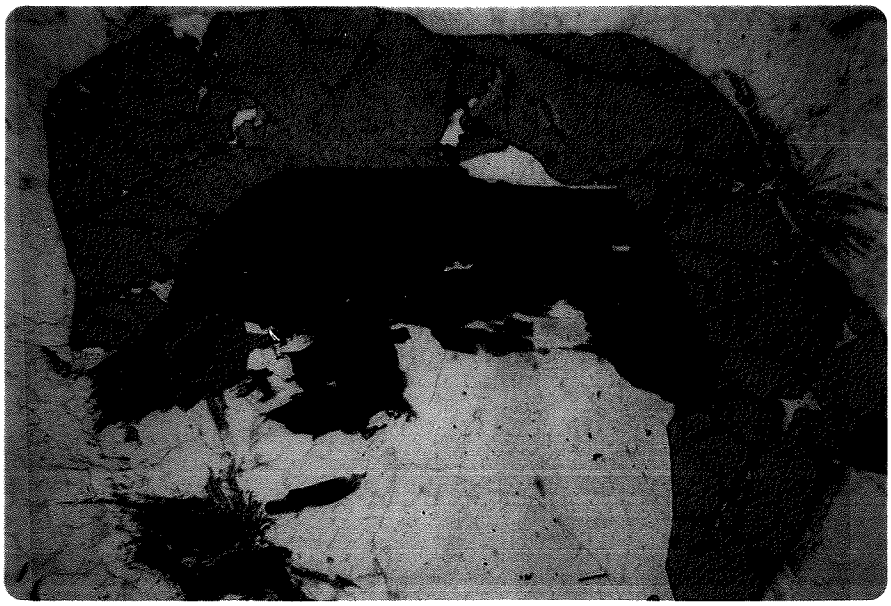

Figure 18. Photomicrograph of association of green biotite and garnet; sillimanite at upper right and lower left; plane transmitted light, X 38. (Location 2).

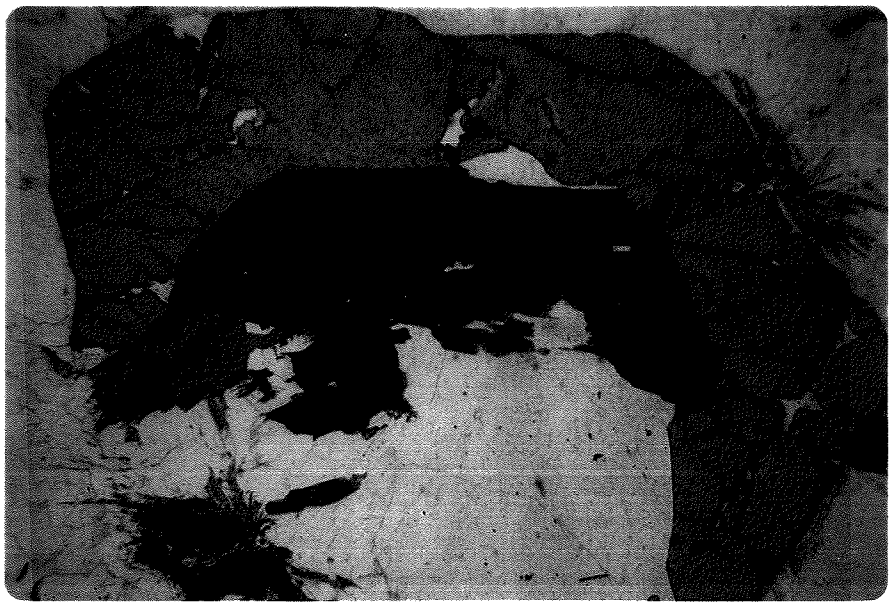

Figure 18. Photomicrograph of association of green biotite and garnet; sillimanite at upper right and lower left; plane transmitted light, X 38. (Location 2).

Figure 19. Photomicrograph of typical leucocratic halo at edge of clot; note myrmekite; crossed nicols, X 38. (Location 2)

CLOTS

The clots mostly have an elongated disc-like shape with the thickness much less than the width and length. Their borders are not sharply defined in thin section, being characterized by the appearande of coarse grained poikiloblastic biotite in the clots and a complete absence of biotite in the immediately adjacent haloes. The clots have the following mineralogy: major biotite, muscovite, quartz, ($\pm$) sillimanite, ($\pm$) garnet, minor hematite, microcline, K-feldspar, rutile, zircon.

The biotite is green in most samples, but is brown in a few. It occurs in clumps of coarse idioblastic grains. The biotite mainly occurs in a diablastic texture with equally coarse grained muscovite. Sillimanite and K-feldspar occur as non-coherent pseudomorphs after biotite. The biotite associated with garnet is mostly green. In part, biotite is patchily replaced by microcline, and at the border between the two minerals a thin rim of muscovite is developed. Fine grained anhedral K-feldspar occurs scattered throughout some of the biotite. An intimate association of green and brown biotite with rutile occurs, which suggests a recrystallization of brown biotite into green biotite. In places, assemblages of biotite, muscovite, and sillimanite are replaced by non-coherent K-feldspar pseudomorphs which cut through the minerals (see Figures 20,21,22).

The muscovite generally occurs as coarse euhedral grains, mostly exhibiting a non-coherent (Figure 3) diablastic replacement relationship with biotite. Together with fine grained K-feldspar, muscovite replaces plagioclase. Thin veins of muscovite (sericite) penetrate large K-feldspar and perthite grains. Muscovite, in turn, is replaced by long unconnected bundles of sillimanite and fine grained skeletal-like grains of K-feldspar. Muscovite may contain disseminated anhedral hematite and very minor rutile.

Quartz occurs as fine to coarse anhedral intersertal grains which may constitute up to 30 percent of the clot. It also occurs as an irregular patchy replacement product of biotite and microcline.

Sillimanite is found in most of the clots. It occurs as coarse bundles of fine grained acicular rods with an associated fine grained

K-feldspar aggregate. These bundles are both coherently and non-coherently pseudomorphous after biotite (Figures 19,20,21).

Garnet is mostly associated with green biotite. It occurs as coarse anhedral to euhedral pink grains. It appears to replace green bioite, as it lies between optically continuous grains of green biotite. The garnet contains fine grained anhedral K-feldspar inclusions.

Hematite occurs as fine grained anhedral inclusions in muscovite and biotite. Anhedral grains of hematite occur associated with brown biotite.

The chemical compositions and Niggli norms of three clots are given in Table II (1-1C, 2-1C, 3-1C).

PARAGNEISS

The paragneisses have a medium grained granoblastic texture with a gneissose structure resulting from alternating leucocratic and melanocratic layers. The leucocratic layers are composed mainly of K-feldspar and quartz with very minor brown biotite (Figure 25). The melanocratic layers are composed of brown biotite, K-feldspar, minor plagioclase and quartz (Figure 24). No sillimanite or garnets were observed in the paragneiss. Biotite schist and amphibolite also occur in the area, but thin sections of these rocks were not made. The chemical compositions and norms of two paragneisses, a biotite schist and an amphibolite are given in Table II.

GRANITES

The granites have a coarse grained crystalloblastic texture with interlocking grains of microcline and quartz and minor fine grained, euhedral, brown biotite.

Chemical compositions of some granitic rocks of the area are given in Table III.

Figure 20. Photomicrograph of green biotite and sillimanite bundles replaced by microcline; plane transmitted light, X 38. (Location 7).

Figure 21. Photomicrograph of green biotite and sillimanite replaced by microcline; plane transmitted light, X 38. (Location 2).

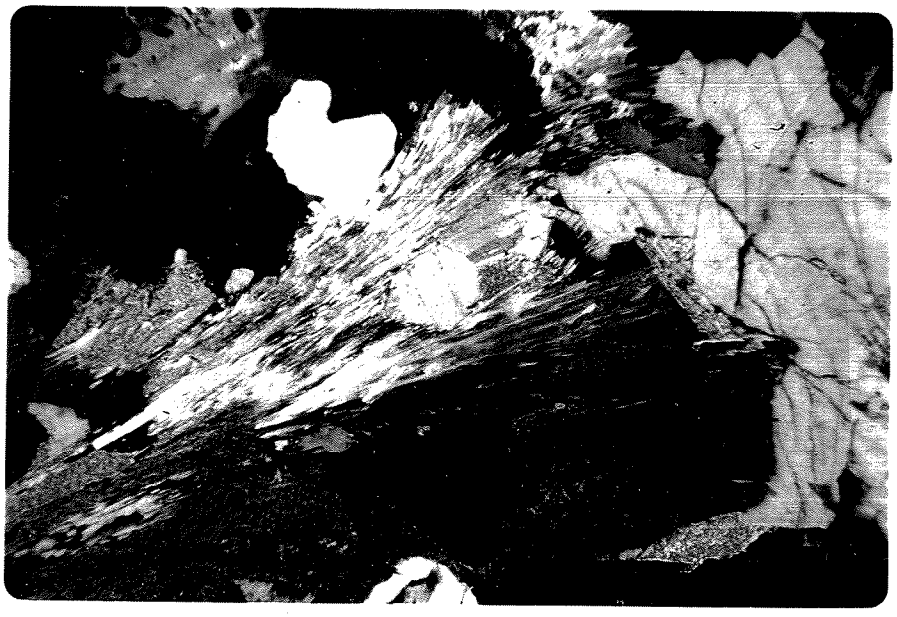

Figure 22. Photomicrograph of green biotite replaced by fibrous sillimanite and then both replaced by microcline; crossed nicols, X 38. (Location 2).

Figure 23. Photomicrograph of intergrowth of green biotite and muscovite; crossed nicols, X 38. (Location 6).

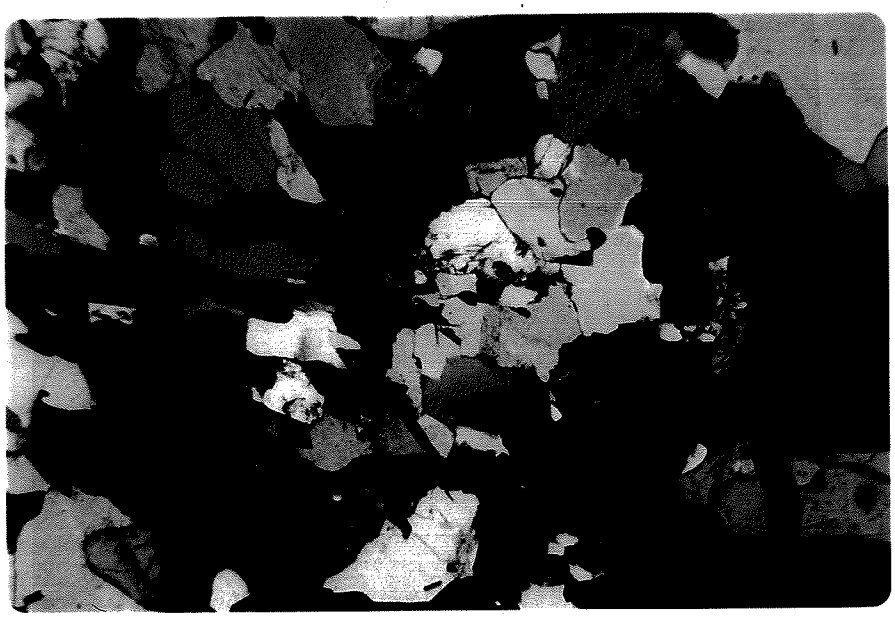

Figure 24. Photomicrograph of biotite-rich layer of paragneiss; note brown euhedral biotite and orthoclase; crossed nicols, X 38. (Location 13).

Figure 25. Photomicrograph of leucosome of paragneiss; note coarse grained crystalloblastic texture of interlocking microcline grains; crossed nicols, X 38. (Location 13).

TABLE II

CHEMICAL ANALYSES:

	1-1C	2-1C	3-2C	20-2	22-3	12-2	13-1
SiO_2	73.15	69.65	60.85	64.40	54.65	59.35	75.60
Al_2O_3	14.36	14.51	16.32	16.68	14.07	17.06	11.73
Fe_2O_3	1.06	1.12	2.20	1.72	8.38	2.03	0.29
FeO	3.87	3.76	3.66	3.39	n.d.	4.11	1.43
MgO	3.78	2.68	6.28	2.92	9.56	4.95	0.69
CaO	0.13	0.61	0.55	2.27	8.96	3.16	2.71
Na_2O	0.30	0.55	0.55	3.85	0.80	3.40	3.48
K_2O	0.88	2.56	5.98	1.76	1.59	2.81	2.92
H_2O	2.05	3.88	3.14	1.28	1.55	1.33	0.36
CO_2	0.07	0.03	0.03	0.10	0.20	0.10	0.06
TiO_2	0.00	0.00	0.19	0.42	0.49	0.54	0.14
P_2O_5	0.12	0.12	0.12	0.25	0.31	0.25	0.17
MnO	0.21	0.05	0.15	0.08	0.18	0.08	0.00
TOTAL	99.48	99.52	100.32	99.12	100.74	99.17	99.58

NIGGLI NORMS:

Calcite	0.19	0.08	0.08	0.26	0.26	0.16
Apatite	0.07	0.27	0.26	0.54	0.53	0.36
Ilmenite	0.00	0.00	0.27	0.60	0.76	0.20
Orthoclase	5.52	16.37	36.79	10.67	16.91	17.67
Albite	2.85	5.33	5.13	35.38	31.01	31.91
Anorthite	0.00	2.22	1.83	9.22	13.65	7.90
Magnetite	1.17	1.26	2.39	1.84	2.15	0.31
Hematite	0.00	0.00	0.00	0.00	0.00	0.00
Corundum	14.93	11.87	9.39	5.73	3.87	0.00
Wollastonite	0.00	0.00	0.00	0.00	0.00	1.73
Enstatite	11.14	8.05	18.16	8.32	14.00	1.96
Ferrosilite	5.56	5.44	4.01	3.54	4.26	1.85
Quartz	58.50	49.11	21.68	23.90	12.60	39.96

LEGEND

1-1C, 2-1C, 3-2C - clots of clotty granites, locations 1, 2, 3 respectively.
20-2 - paragneiss, location 20.
22-3 - biotite schist, location 22.
12-2 - amphibolite, location 12.
13-1 - paragneiss, location 13.

Analysts - K. Ramlal, University of Manitoba and J. Morin.

TABLE III

CHEMICAL ANALYSES:

	17-1	20-1	21-1	23-1
SiO_2	73.05	73.05	75.10	74.65
Al_2O_3	13.83	14.26	13.27	13.67
Fe_2O_3	0.16	0.53	0.19	0.39
FeO	0.18	0.74	0.58	0.37
MgO	0.03	0.53	0.31	0.18
CaO	0.25	0.82	0.60	0.60
Na_2O	2.75	3.13	3.25	3.25
K_2O	9.13	5.84	5.24	5.68
H_2O	0.15	0.48	0.48	0.22
CO_2	0.11	0.08	0.31	0.16
TiO_2	0.00	0.05	0.03	0.00
P_2O_5	0.15	0.18	0.17	0.17
MnO	0.00	0.01	0.00	0.00
TOTAL	99.79	99.70	99.53	99.34

LEGEND

17-1 - coarse grained pink granite, location 17.

20-1, 21-1, 23-1 - medium grained pink granites, locations 20, 21 and 23 respectively.

Analysts - K. Ramlal, University of Manitoba and J. Morin.

M I N E R A L O G Y

ALKALI FELDSPARS

An estimate of the variation in the Al-Si disorder of the K-feldspars was obtained by a triclinicity study. As defined by Goldsmith and Laves (1954), the triclinicity is $\Delta = d(131) - d(1\bar{3}1)$. Orthoclase yields a value of $\Delta = 0.0$, while triclinic microcline has $\Delta = 1.0$. Thus an estimate of the Al-Si disorder from orthoclase to microcline can be made.

A useful variation of the measurement technique for relatively impure K-feldspar separates with albite has been devised by Parsons (1965). He found that with his relatively sodic rocks, albite peaks interfered with the measurement of the $1\bar{3}1$ peak of microcline. To overcome this problem, he constructed a graph illustrating the linear dependence of the 2θ values for (131) and $(1\bar{3}1)$ reflections with d separation,(i.e. $d(131) - d(1\bar{3}1)$). Utilizing this graph, one needs only the (131) reflection peak to calculate the triclinicity. In the present study, use has been made of Parson's graph because of the relatively high content of albite imputities in some of the separates.

Triclinicity values were obtained for samples of the clotty granite, pegmatite, granite and paragneiss. The values are listed in Table IV. The data shows three groupings:

(1) $\Delta = 0.0$ to 0.4 orthoclase of the paragneiss;

(2) $\Delta = 0.4$ to 0.7 intermediate microcline of the clotty granite and pegmatites;

(3) $\Delta = 0.7$ to 1.0 intermediate to maximum microcline of the granites.

Nilssen and Smithson (1965) have discussed some of the interpretations of triclinicity values. It is generally accepted that low values correspond to a high temperature formation and/or low growth kinetics, while high values correspond to lower temperatures of formation and/or faster growth kinetics. An increase in volatile content increases the rate of the orthoclase to microcline transformation.

TABLE IV

ROCK TYPE	SAMPLE #	TRICLINICITY
Clotty granite	11-3	0.62
	7-1	0.66
	10-1	0.62
	11-2	0.66
	14-1	0.77
Pegmatite	1-2	0.56
	1-4	0.65
	1-3	0.62
Granite	15-1	0.66
	16-1	0.97
	17-1	0.65
	18-1	0.97
	19-1	0.68
	20-1	0.95
	21-1	1.0
	22-1	0.21
	23-1	0.82
Paragneiss	13-1 (paleosome)	0.0
	13-1 (leucosome)	0.67
	22-2 (whole rock)	0.0

Triclinicity values calculated from the graph of Parsons (1965).

Thus, the temperature of formation and the volatile content are two of the main factors affecting triclinicity values. Since the rocks were all at the same depth in the crust, they probably reached the same maximum temperature. Assuming that temperature differences were negligible, the volatile content might explain the observed triclinicities. This would indicate that the paragneiss had a low volatile content compared to a relatively high volatile content in the clotty granite, pegmatites and granites.

In one of the paragneisses (Sample 13-1), disequilibrium between alkali feldspars is indicated (Figures 22,23). The alkali feldspar of the paleosome is medium grained orthoclase (Δ =0.0), but a thin leucosome is present in which the alkali feldspar is coarse grained crystalloblastic M-twinned microcline. If the leucosome was intrusive, a higher volatile content in it might explain the apparent disequilibrium. If this assumption is correct, it indicates that microcline can exist at the high temperatures of the orthoclase stability field if a high enough volatile content is present or that the orthoclase formed is persisting metastably in the paragneiss.

BIOTITE

The composition of biotites reflects the reaction and P-T-X conditions. Hayama (1958), studied the colour of biotites in metamorphic rocks and found it to depend mainly on the TiO_2 content and Fe_2O_3 / (Fe_2O_3 + FeO) ratio. He concluded that a higher Fe_2O_3 / (Fe_2O_3 + FeO) ratio and lower TiO_2 content gives a green colour to the biotite, while a lower Fe_2O_3 / (Fe_2O_3+FeO) ratio and higher TiO_2 content gives the biotite an increasingly brown colour.

Likewise, Chinner (1960), in his study of pelitic gneisses from Glen Cova, found that green biotite was restricted to rocks with a high oxidation ratio (hematite-bearing), while brown biotite was restricted to rocks with lower oxidation ratios. He also found that the ratio MgO/(MgO+FeO), and the content of TiO_2, in biotite increases with increasing rock oxidation ratio, thus reflecting increased oxidation of the FeO component to Fe_2O_3.

Loberg (1963), in a study of a "flecky gneiss" in Sweden which is very similar to the clotty granite, found that the brown colour of the biotites was due to their high Ti content, relative to the low Ti content of the green biotite.

The relationship between biotite colour and TiO_2 content is seen in thin sections of some of the clots and of the paragneisses. In specimen No. 5-1 of the clotty granite (see Figure 26), the components of the following reaction were observed:

brown biotite $\longrightarrow$ green biotite + rutile

In this specimen, all the biotite in the clots are brown, except at one of the clot edges where rutile and green biotite were observed coherently pseudomorphous after the brown biotite. A similar relationship was also observed in one of the gneisses studied.

Three kinds of biotite were observed in the thin sections:

(1) fine grained euhedral brown biotite occurring in the clotty granite matrix, granites and gneisses;

(2) coarse grained brown biotite occurring in some of the clots of the clotty granite;

(3) coarse grained green biotite occurring in some of the clots of the clotty granite.

Analyses were made of three different biotites: 1-1 matrix brown biotite of the clotty granite, 22-2 brown biotite of a biotite schist, 1-1 clot green biotite of the clotty granite (see Table VI). The relationships can be seen on the accompanying diagrams (Figure 27).

The brown biotites both have very high TiO_2 contents compared to the green biotite (2.41 and 2.20 vs. 0.17 weight percent). The green biotite has a lower oxidation ratio (15.3) than the brown biotite of the matrix (21.9) and the brown biotite of the schist (24.6). This suggests that the high TiO_2 difference masks any effect that the oxidation ratio exerted on the colour.

The data agrees well with Saxena (1967), who found that the Ti concentration increases as the Al concentration decreases. When plotted on the ternary diagram MgO-FeO-Al_2O_3, the Ti-rich biotites have less Al_2O_3 than the Ti-poor biotite. Even though the Ti-rich biotites differ in FeO and MgO contents, their sums are almost equal and thus illustrate

Figure 26. Photomicrograph of colour-zoned biotite; brown biotite in centre and green biotite at edges; also disseminated rutile and hematite; plane transmitted light, X 76. (Location 5).

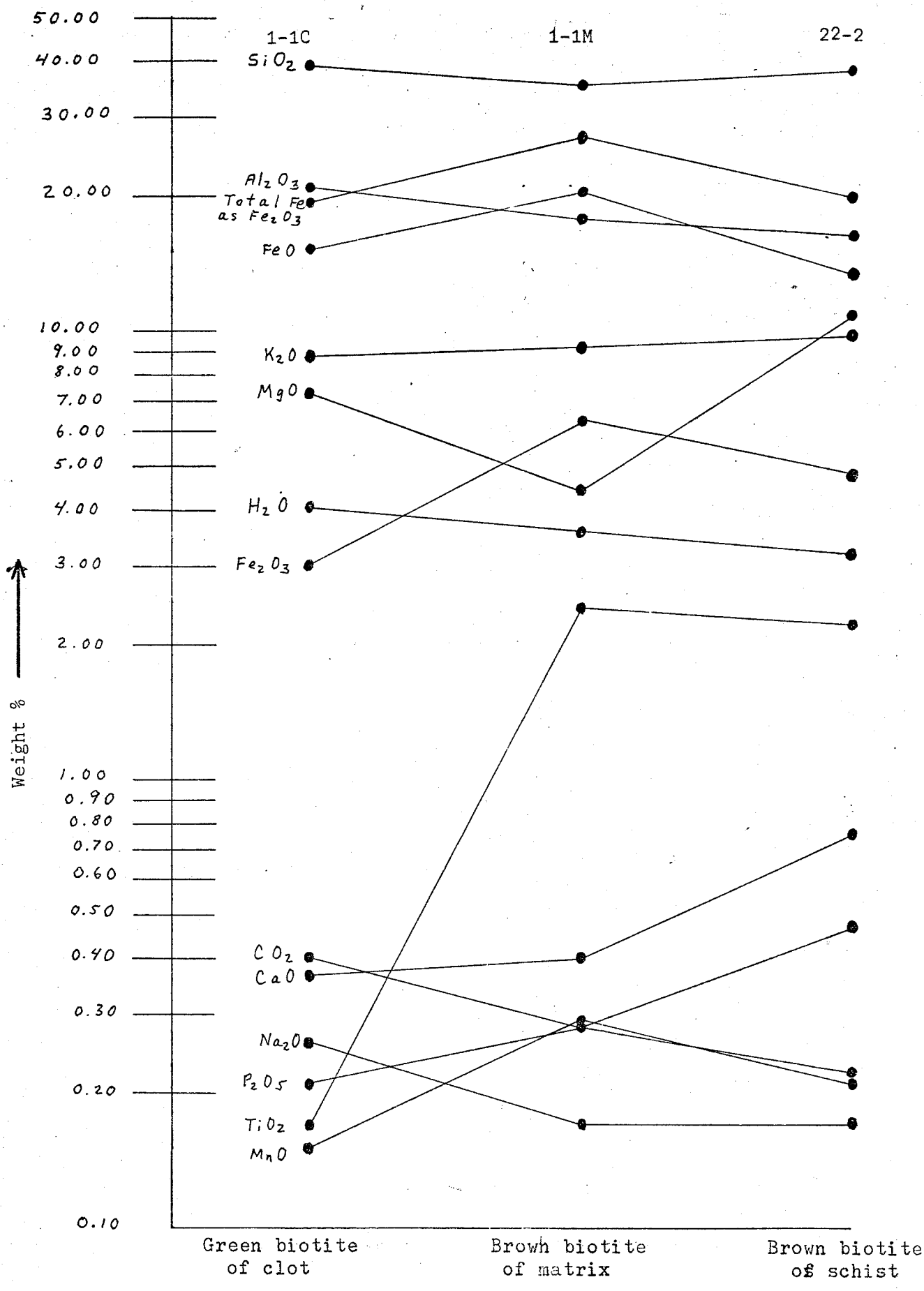

Figure 27. Logarithmic plot of chemical analyses of biotites of Table V.

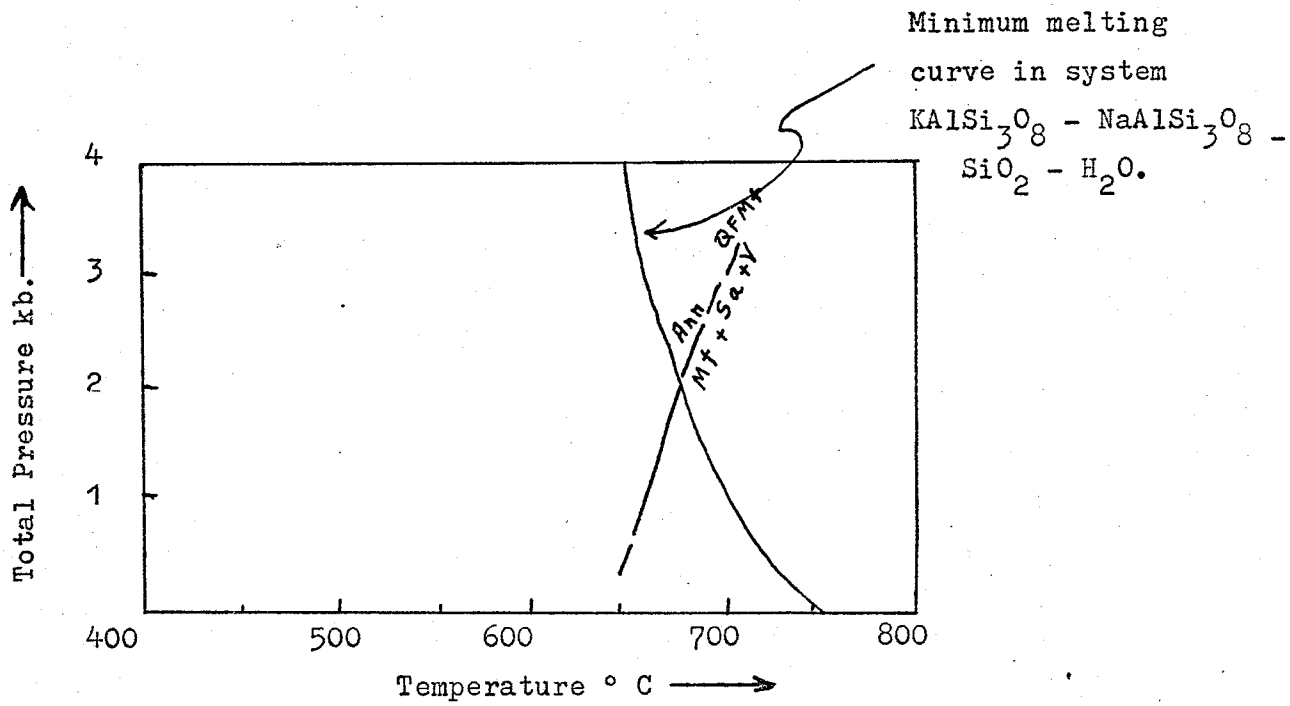

Figure 28. P - T diagram for the iron-biotite - alkali feldspar system (Rutherford, 1969).

Q F Mt = quartz - fayalite - buffer

Ann = annite

Mt + Sa + V = magnetite + sanidine + vapour.

the Fe^{+2} - Mg^{+2} diadochy. Also, the green biotite has a higher Na_2O content than the brown biotites and this is consistent with the proposed origin. Thus, the effect of TiO_2 on the biotite colour agrees well with the findings of other investigators.

The P-T-X conditions which resulted in the alteration of the brown biotite may be an increased P_{H_2O} and an increase in the concentration of Na in the intergranular film. Relative to K, Na shows both a higher rate of dissolution in water (Khitarov, 1953, 1957), and a greater mobility in water (LeClerc, 1956). Orville (1963) also showed that with an increase in temperature, the K / K+Na ratio in the vapour phase that coexists with two alkali feldspars decreases with an increase in temperature, so that at higher temperatures, the vapour phase would be relatively depleted in K relative to Na. Thus, it is probable that with the relatively high sodic composition of the gneisses, the intergranular film would be more sodic than potassic.

In his study of the iron biotite - alkali feldspar system, Rutherford (1969) found that an increase in the concentration of Na in the silicate melt lowered the temperature stability field of iron-rich biotite. This is due to the substitution of Na for K in the biotite structure. To regain equilibrium with the melt, the biotite would have to decrease its Fe^{+2} / Mg^{+2} ratio. In the present study, the brown biotite of the matrix has a greater FeO / MgO ratio (6.2) than the green biotite (2.5). Besides losing Fe and gaining Mg, the brown biotite lost Ti in the reaction. Also in accordance with this hypothesis is the greater content of Na_2O and lower content of K_2O in the green biotite than in the brown biotite (Figure 27).

The brown biotite of the matrix crystallized from a melt. According to Rutherford (1969), an iron-rich biotite could not crystallize from a granitic liquid below P_T = 4 kb. (Figure 28). This gives a reliable estimate for the minimum P-T conditions reached, ie. P = 4 kb. and T = 640° C. However, Rutherford notes that the presence of titanium in the biotite may raise the stability field of an iron biotite to higher temperatures.

GARNET

Garnets occur scattered throughout the clotty granite, including the clots, the matrix and the pegmatites. They are pale red, medium grained, euhedral to anhedral grains which show a replacement relationship with biotite (Figure 18). Rickwood (1968) has devised a method of calculating a garnet in terms of its end-members, and his method has been applied to the one chemical analysis of garnet from Sample 2-1. Dwibedi (1966) has calculated a garnet composition from a granitic rock along the Red Lake Road south of Cliff Lake in terms of the pyralspite molecules by the unit cell edge - refractive index - specific gravity method. Both results are given in Table V

T A B L E V

	2-1	94a
Almandine	75.2	69.4
Spessartine	11.4	2.2
Pyrope	10.1	28.4
Andradite	3.3	n.d.
	100.0	100.0

LEGEND

2-1 - Garnets separated from whole rock sample 2-1 .

94a - Garnets separated from Dwibedi's sample 94a (1966); sample located south of Cliff Lake along Red Lake Road.

TABLE VI

CHEMICAL ANALYSES:

	1-1C Biotite	1-1M Biotite	22-2 Biotite	1-3 Feldspar	2-1 Garnet
SiO_2	38.80	35.10	37.50	63.10	37.25
Al_2O_3	20.95	17.74	16.05	19.15	19.66
Fe_2O_3	3.04	6.31	4.78	0.42	3.36
FeO	15.09	20.28	13.18	n.d.	30.10
MgO	7.25	4.40	10.80	n.d.	2.23
CaO	0.37	0.40	0.75	n.d.	1.01
Na_2O	0.26	0.17	0.17	7.09	0.06
K_2O	8.80	9.10	9.68	10.74	0.10
H_2O	4.05	3.55	3.18	n.d.	0.20
CO_2	0.40	0.28	0.22	0.00	0.00
TiO_2	0.17	2.41	2.20	0.00	0.00
P_2O_5	0.21	0.28	0.47	0.00	0.33
MnO	0.15	0.29	0.21	0.01	4.40
TOTAL	99.54	100.31	99.19	100.51	98.95

LEGEND

1-1C - green biotite from clot of clotty granite 1-1.

1-1M - brown biotite from matrix of clotty granite 1-1.

22-2 - brown biotite of biotite schist.

1-3 - alkali feldspar from pegmatite.

2-1 - garnet from clotty granite 2-1.

Analysts - K. Ramlal, University of Manitoba and J. Morin.

CHEMICAL TRENDS

Results of the chemical analyses of the rocks of the study area (Tables I, II,III) were plotted on various diagrams to aid in the petrogenetic interpretation.

Alkali Plot

A triangular variation diagram was constructed to show the variation in the relative distribution of the weight percentages of CaO, Na_2O and K_2O (Figure 29). The paragneisses, clotty granites and granites, with one exception, occupy distinctly separated areas on the diagram. The clotty granites lie intermediate between the paragneisses and the granites. A trend seems to be present from the paragneiss to the granites that involves a progressive increase in K_2O and decrease in CaO. The granites also appear to be relatively depleted in Na_2O compared to the paragneisses and the clotty granites.

Alkali - F - M Plot

An Alkali - F - M diagram was also constructed. In his study of granites in California, Ross (1969), found it to be the best plot graphically presenting oxide data without showing the influence of silica (Figure 30). In addition to the rocks of the study area, the granitic rocks along the Red Lake Road studied by Dwibedi (1966) were also plotted. As observed on the diagram, the clotty granites and granites of the area are higher in alkali oxides and lower in mafic oxides than the paragneisses.

Quartz - Albite - Orthoclase Plot

In Figure 31, the molecular proportions of normative quartz, albite and orthoclase are plotted on the ternary diagram Q - Ab - Or. The normative salic compositions of the two paragneisses are also plotted. According to James and Hamilton (1969), the normative salic composition represents the composition of the melt formed by the melting of all the salic components of a rock. Thus, the normative salic composition represents the composition end salic melt, while the more Q - Or-rich melts represent the compositions of the earlier formed melts. Also

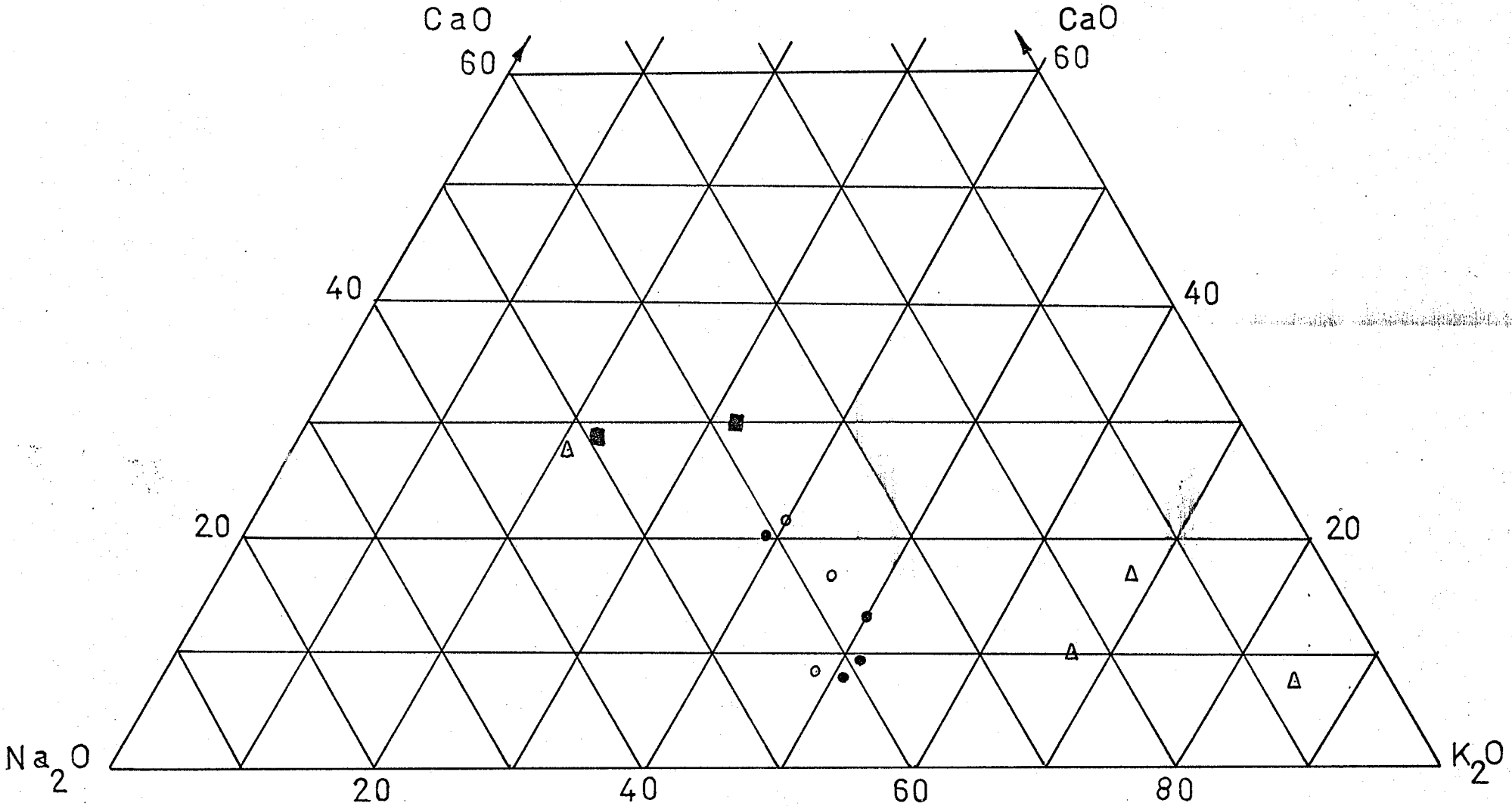

Figure 29. $CaO-Na_2O-K_2O$ variation diagram. Clotty granite matrix (o); clotty granite (•); granites of area (Δ); paragneiss (■). Plotted as weight percentages.

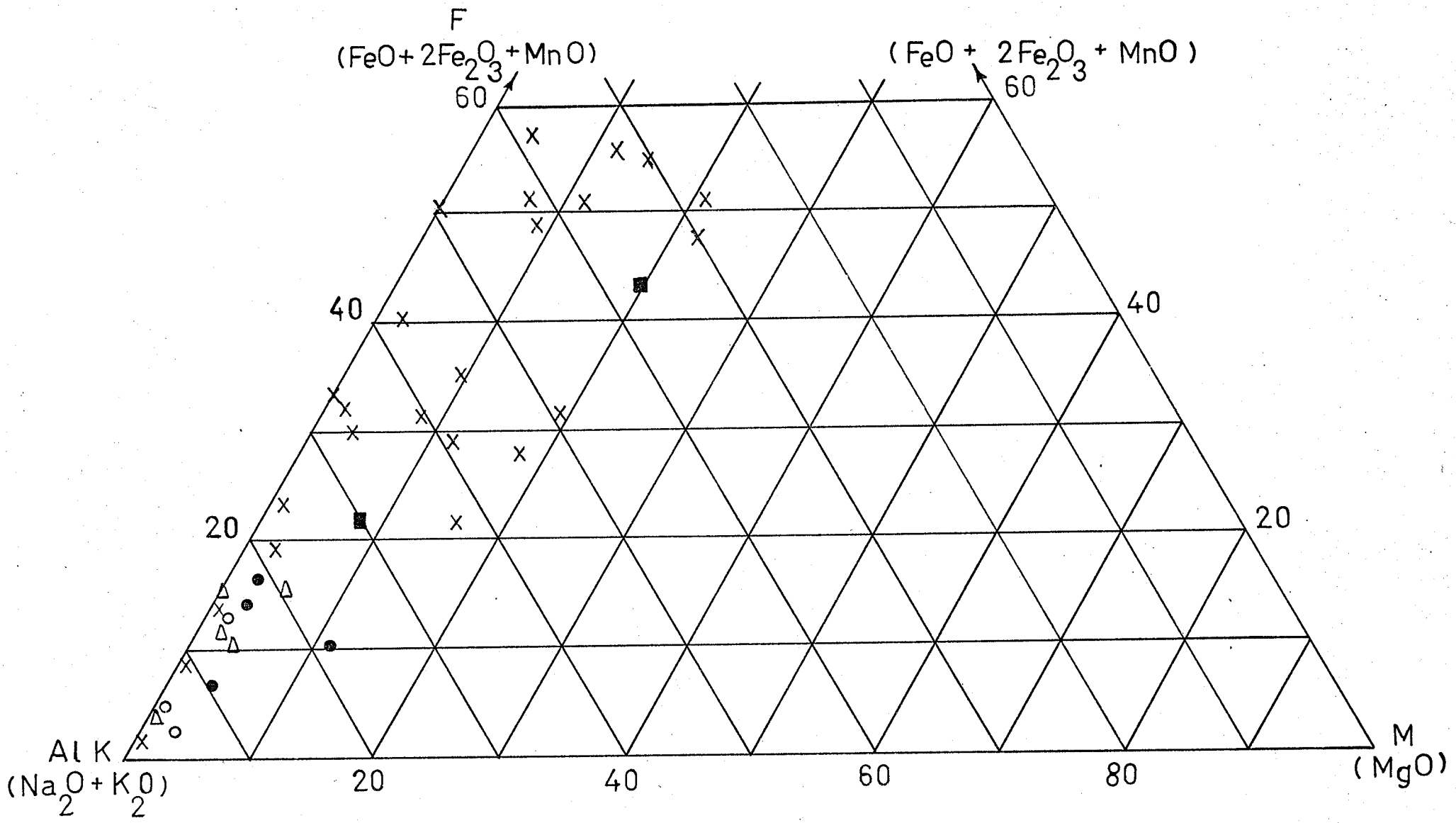

Figure 30 Alkali-F-M diagram. Clotty granite matrix (o); clotty granite (●); paragneiss (■); granitic rocks along Red Lake Road (x); granites of study area (Δ). Plotted as weight percentages.

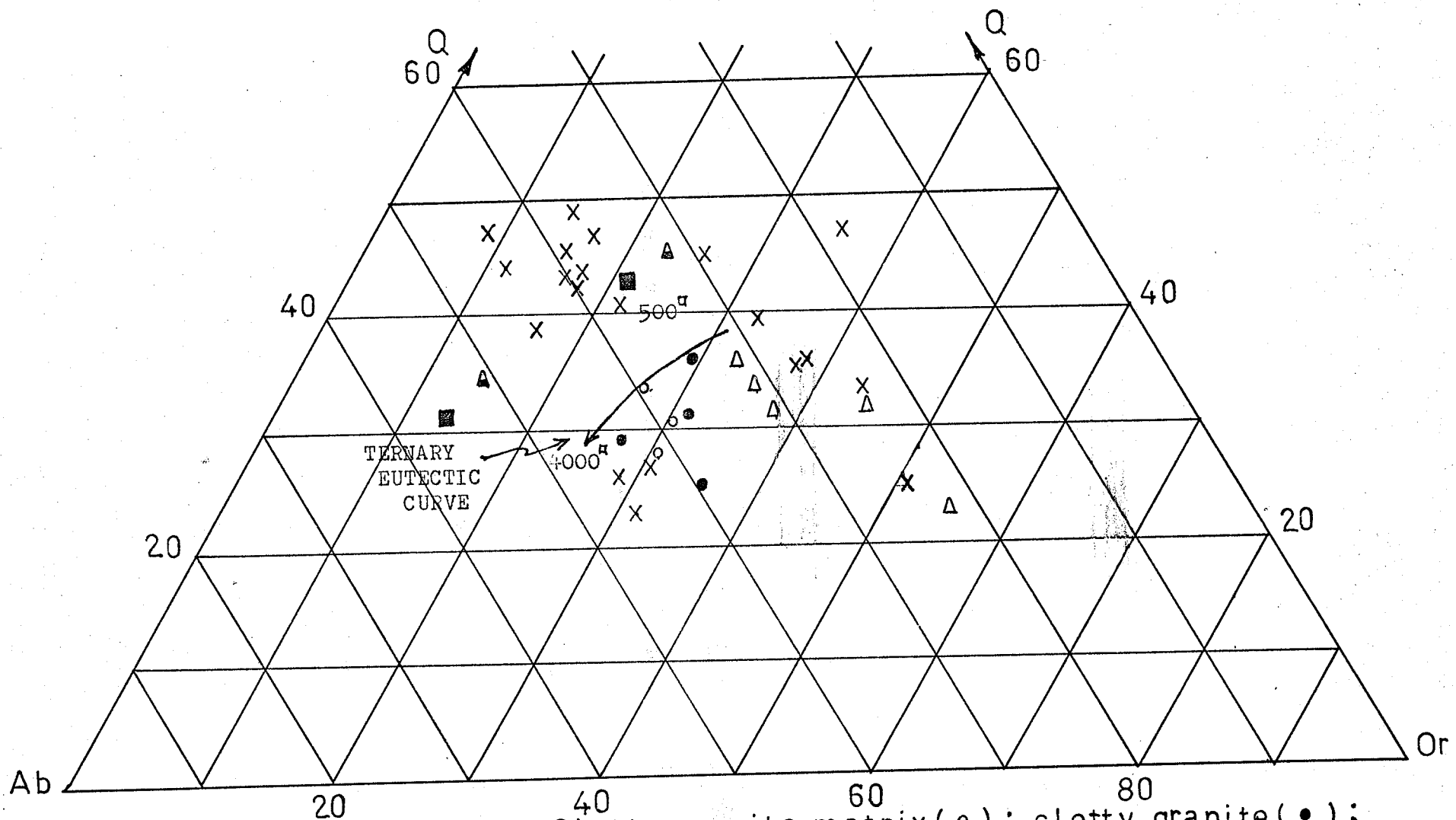

Figure 31. Q-Ab-Or diagram. Clotty granite matrix (o); clotty granite (•); paragneiss (■); normative salic (▲); granitic rocks along Red Lake Road (x); granites of study area (Δ). Plotted as normative molecular % proportions.

shown on the diagram is the minimum eutectic composition curve with P_{H_2O} varying from 500 bars at the higher Q end to 4000 bars (Tuttle and Bowen, 1958). The curve describes the locus of migration of the ternary eutectic of the Q - Ab - Or system with varying P_{H_2O}. Data taken from partial melting experiments (Winkler, 1968) were used to plot the trends of the minimum temperature melt compositions derived from partially melted granitic composition rocks. The curves vary with P_{H_2O}, Ab / An ratio, P_{Vap} and concentration of HCl.

The paragneisses, clotty granites and granites of the area form distinct fields on the diagram. The clotty granites and granites of the area fall below the eutectic curve on the Or-rich side. The clotty granite falls in a field governed by curves of minimum melting compositions derived by partial melting, especially at higher P_{Vap} and P_{H_2O} and higher Ab / An ratios.

The granitic rocks along the Red Lake Road studied by Dwibedi (1966) were also plotted on the Q - Ab - Or diagram (Figure 31). The plots may be separated into three fields that correspond to the fields described above. Some of the rocks that Dwibedi describes as granitic, fall into the paragneiss field, and they are interpreted to be almost completely melted gneisses. The granitic rocks in the Or-rich field correspond quite well with the field occupied by the granites of the study area. The rocks in the Or-rich field theoretically cannot have been derived mainly by crystallization from a melt, because they plot too far from the minimum melting and eutectic crystallization paths. It is suggested that they have resulted from K-metasomatism.

Anorthite - Albite - Orthoclase Plot

An An - Ab - Or diagram was constructed on which was plotted the molecular proportions of normative anorthite, albite and orthoclase for rocks of the study area and the granitic rocks of Dwibedi (1966), (Figure 32). The boundary curve in the diagram separates the fields of plagioclase and alkali feldspar . The curve has been projected from the quartz saturated surface onto the ternary feldspar face at 1000 bars P_{H_2O}, and the liquidus relations as drawn are considered to be only approximate (James and Hamilton, 1969). The temperature at the liquidus decreases as the An content in the liquid decreases.

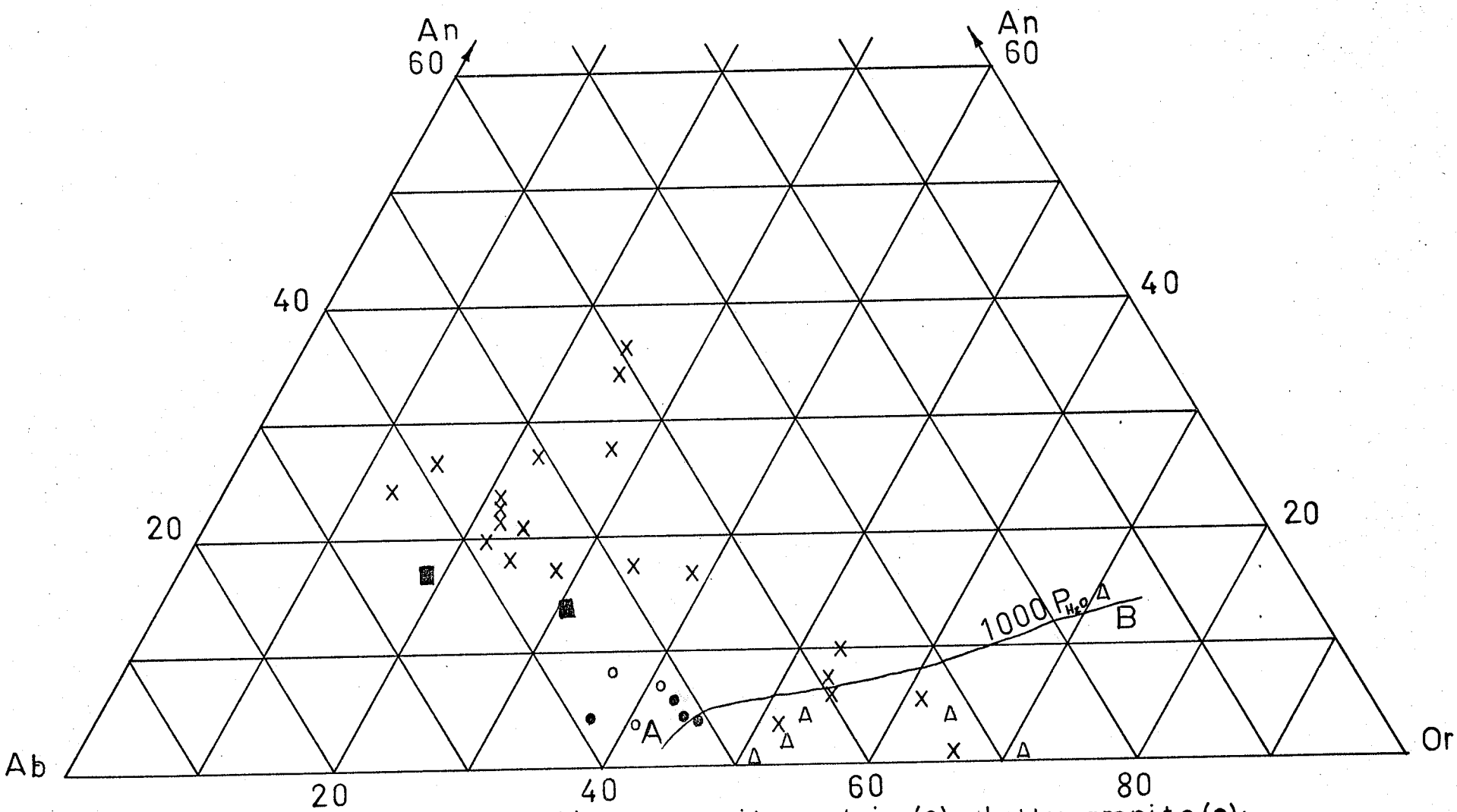

Figure 32. An-Ab-Or diagram. Clotty granite matrix (o); clotty granite (●); paragneiss (■); granitic rocks along Red Lake Road (x); granites of study area (Δ). Two-feldspar-quartz saturated boundary curve A-B at 1000 P_{H_2O} shown, (James and Hamilton, 1969). Plotted as normative molecular % proportions.

The clotty granites and other granites of the study area appear to be separated from each other by the boundary curve. The clotty granites lie on the plagioclase side of the liquidus, while the granites lie on the alkali feldspar side.

The granitic rocks along the Red Lake Road likewise may plot in two fields, one on either side of the boundary curve. The Or-rich field may represent a minimum melt composition, derived from the early partial melting of gneisses and then subjected to K-metasomatism, while the An - Ab -rich field may represent a product of more complete partial melting.

Barth (1966) points out that the CIPW norms are not the most accurate norms to use in these crystallization diagrams because they do not account for the K_2O in the biotite. Thus, the norms are biased to a higher concentration of Or, especially the more biotite-rich rocks such as the clotty granites. However, the amount of biotite in these rocks (maximum five percent) does not appear to be large enough to significantly affect Figures 31 and 32.

INTERPRETATION OF RESULTS

The clotty granite is interpreted to be the product of the partial anatexis of a paragneiss. The following points are indicative of this origin: layering, mineralogy, association, experimental work and chemical data.

Layering in the clotty granite in some areas is suggestive of gneissic layering (Figure 7). The clot layers appear to represent disintegrated biotite-rich layers or melanosomes of the paragneiss (Figure 12), with the distance between layers similar to that of the gneisses. During intrusion, the layering has been gently folded in places (Figures 5 and 7). The mineralogy of the clots and matrix is similar to that of the melanosomes and leucosomes respectively of the paragneisses.

The clotty granite lies in an area that was subjected to high temperature regional metamorphism (Dwibedi, 1966). The area to the south has been metamorphosed to the granulite facies and the area to the north to the lower amphibolite facies. The intermediate to maximum microcline present in the rocks suggests that the granite is synkinematic to late kinematic (Marmo, 1958). The gneisses of the English River Gneissic Belt have been interpreted to have formed deep within the crust in an orogenic zone, and according to Dwibedi (1966), anatexis was prevalent.

Observed distribution of the granitic rocks in triangular diagrams agrees with results of experimental work on partial melting by Winkler and Von Platen (Winkler, 1967). The clotty granite is more potassic than the neighbouring gneisses, as would be expected for a product of partial melting. However, it is less potassic than the nearby granites which are considered to have been derived at the earlier stages of partial melting. The clotty granite and nearby granites contain less mafic components than the paragneisses, indicating that during anatexis the higher melting point mafic components were depleted by separation from the melts.

Temperatures present in the lower part of an orogenic zone are high enough to initiate the melting of the low melting-point components of rocks. The leucosomes of the gneisses would be the

first to melt and the P_{H_2O} would increase in response to the volume of liberated, formerly trapped, intergranular and intragranular water. However, it is equally possible that a local relatively high concentration of H_2O migrated into the area and that this correspondingly increased the amount of melt that could form.

The intergranular fluid medium may be expected to have been relatively rich in Na because of the relatively high Na / alkali ratio of the paragneisses. Due to the increase in the concentration of Na and in P_{H_2O} some of the brown biotite of the clots altered to green biotite with release of rutile and hematite. Subsequent to this, and with a further increase in P_{H_2O}, the biotite was partly replaced by muscovite. The P - T conditions prevailing, and the alkali-rich melt present, promoted the following composite reactions:

brown biotite + Na^+ $\longrightarrow$ green biotite + rutile + hematite

biotite $\longrightarrow$ garnet + K-feldspar + sillimanite + hematite + cordierite

muscovite + quartz $\longrightarrow$ sillimanite + K-feldspar

In these reactions, the $Fe^{+2,+3}$, Mg^{+2}, and Mn^{+2} of biotite went to form garnet, hematite and possibly cordierite.

The interpreted result of the increased temperature and P_{H_2O} was a melt in which scattered mafic clots were enclosed which intruded into overlying gneisses. The mixture experienced a decrease in temperature which initiated crystallization of the melt. Flow structures were formed in the semi-fluid medium during intrusion.

Crystallization of the matrix proceeded with the precipitation of euhedral brown biotite crystals. Plagioclase crystallized with minor inclusions of biotite. Quartz dihexahedra crystallized from the silicate melt subsequent to plagioclase. As the crystallization proceeded, the concentration of the aqueous fluid increased relative to the silicate melt, and a point was reached at which crystallization occurred from both. The silicate melt yielded the granitic matrix and the aqueous fluid yielded the much coarser grained, irregular trending pegmatite phases. This stage of crystallization resulted in the precipitation of alkali feldspar and quartz.

The last stages of crystallization were concerned with the aqueous fluid. The role of this residual fluid was to promote growth of large crystals, physical segregation of the growing crystalline phases (Figures 10 and 11), and reaction between crystalline and fluid phases (Jahns and Burnham,1969). An increase in the amount of volatiles is reflected in the increased alkali diffusion rate as indicated by thickened albite exsolution lamellae near the edges of some perthite grains (Figure 17). The large poikiloblastic K-feldspar megacrysts are also evidence of the increased rate of diffusion made possible by the aqueous fluid. Muscovite, biotite, and sillimanite were replaced in part by K-feldspar during this stage. The K-feldspars, biotite and plagioclase were subjected to very minor sericitization and, in places, to replacement by muscovite.

The leucocratic haloes round the clots (Figure 5) may be the result of the precipitation of alkali feldspars and quartz at the margins of the clots. This type of formation is found in pegmatites, where the aqueous fluid precipitates at the margins of xenoliths of quite different composition (Jahns and Burnham, 1969).

Another theory that has been suggested to account for the origin of the clots involves the pseudomorphic replacement of cordierite by biotite and sillimanite. Cerny (Personal communication, 1970) studied biotite - sillimanite knots near a granite contact and found them to be pseudomorphous after cordierite. Cordierite is however, a rare mineral in the clotty granite. It was noted only in the clotty granite at locality 4, and it did not occur in any of the thin sections made, nor was its presence determined in any of the samples taken.

The occurrence of cordierite is considered to be due to the prograde regional metamorphism of biotite. It would thus be genetically dissimilar to the contact metamorphic feature studied by Cerny,

A C K N O W L E D G M E N T S

The author gratefully acknowledges the financial assistance of the Department of Earth Sciences, University of Manitoba, and the Geological Survey of Canada. Expenses for field work were paid by Geological Survey of Canada Grant 40-66 (to A. C. Turnock). Helpful discussions, guidance and field assistance were received from A. C. Turnock and G. S. Clark. Miss V. Semochuk assisted in the field work. The author received guidance and benefited from discussions with R. B. Ferguson and P. Cerny. Assistance with the chemical analyses was provided by K. Ramlal and R. Hill. The thin sections were made by Miss I. Berta. Encouragement, helpful discussions and field assistance by the author's wife, Mrs. M. Morin, are gratefully acknowledged.

REFERENCES

BARTH, T. F. W., (1966): Aspects of the crystallization of quartzo-feldspathic plutonic rocks; Tschermaks Mineral. Petrog. Mitt. 11, 209-222.

CERNY, P., (1970): Personal communication.

CHINNER, G. A., (1960): Pelitic gneisses with varying ferrous / ferric ratios from Glen Cova, Angus, Scotland; J. Petrol. 1, 178-217.

DWIBEDI, K., (1966): Petrology of the English River Gneissic Belt; Unpublished PhD. thesis, University of Manitoba, Winnipeg, Manitoba.

GOLDSMITH, J. R. and LAVES, F. (1954): The microcline stability relations, Geochem. Cosmochim. Acta. 5, 1-19.

JAHNS, R. H. and BURNHAM, C. W. (1969): Experimental studies of pegmatite genesis: 1 - A model for the derivation and crystallization of granitic pegmatites; Econ. Geol. 64, 843-864.

JAMES, R. S. and HAMILTON, D. L. (1969): Phase relations in the system $NaAlSi_3O_8$ - $KAlSi_3O_8$ - $CaAl_2Si_2O_8$ - SiO_2 at 1 kilobar water vapour pressure; Contrib. Mineral & Petrol.

HAYAMA, Y. (1959): Some considerations on the colour of biotite and its relation to metamorphism; Jour. Geol. Soc. Japan 65, 21-30.

KHITAROV, N. I. (1957): The chemical properties of solutions arising as a result of the interaction of water with rocks at elevated temperatures and pressures; Geochemistry (U.S.S.R.) (English Transl.) 6, 481-492.

LECLERC, P. (1956): Caracteres de diffusion des ions mobiles dans le reseau vitreaux; Trav. 4c Cong. Intern., Verre, Paris, 331-335.

LOBERG, B. (1963): The formation of a flecky gneiss and similar phenomena in relation to the migmatite and vein gneiss problem, Geo. Foren.,Stockholm, Forh., 85, 1-109.

MARMO, V. (1958): Orthoclase and microcline granites;;Am. J. Sci. 256, 360-364.

NILSSEN, B. and SMITHSON, S. B. (1965): Studies on the Precambrian Herefoss granite; 1. K-feldspar obliquity; Norsk Geo. Tidsskr. 45, 367-396.

ORVILLE, P. M. (1963): Alkali ion exchange between vapour and feldspar phases; Am. J. Sci. 261, 201-237.

PARSONS, I. (1965): The feldspathic syenites of the Loch Ailsh Intrusion, Assynt, Scotland; J. Petrol. 6, 365-395.

RICKWOOD, P. C. (1968): On recasting analyses of garnet into end-member molecules; Contbr. Mineral. and Petrol. 18, 175-198.

ROSS, D. C. (1969): Descriptive petrography of three large granitic bodies in the Inyo Mountains, California; U. S. G. S. Prof. Paper 601.

RUTHERFORD, M. J. (1969): An experimental determination of iron-biotite - alkali feldspar equilibria; J. Petrol. 10, 381-408.

SAXENA, S. K. (1967): Intracrystalline chemical variations in certain calcic pyroxenes and biotites; N. Jb. Miner. Alb. 107,# 3, 299-316.

TUTTLE, O. F. and BOWEN, N. L. (1958): Origin of granite in the light of experimental studies in the system $NaAlSi_3O_8$ - $KAlSi_3O_8$ - SiO_2 - H_2O; Geol. Soc. Am. Mem. 74, 1-153.

WILSON, H. D. B. and BRISBIN, W. C. (1963): Nature of the granitic crust in the Superior Province; Abstract, Geol. Soc. Am. 76 th Annual Meeting, November 1963,p. 180A.

WINKLER, H. G. F. (1967): Petrogenesis of Metamorphic Rocks, 2nd ed. Springer, Berlin, 218 pp.